Available online at www.sciencedirect.com
ScienceDirect
Journal of Solid State Chemistry 180 (2007) 1708–1712
JOURNAL OF SOLID STATE CHEMISTRY
www.elsevier.com/locate/jssc

Syntheses and characterization of zero-dimensional molybdoantimonites, $A_2(Mo_4Sb_2O_{18})$ (A = Y, La, Nd, Sm, Gd and Dy)

G. Kalpana, K. Vidyasagar*

Department of Chemistry, Indian Institute of Technology Madras, Chennai 600 036, India

Received 7 February 2007; received in revised form 17 March 2007; accepted 22 March 2007
Available online 28 March 2007

Abstract

Six new isostructural $A_2(Mo_4Sb_2O_{18})$ (A = Y, La, Nd, Sm, Gd and Dy) compounds have been synthesized by solid-state reactions and characterized by single crystal X-ray diffraction and spectroscopic techniques. They crystallize in $C2/c$ space group with 4 formula units and contain A^{3+} cations and discrete centrosymmetric anionic $(Mo_4Sb_2O_{18})^{6-}$ aggregates, made of tetrahedral MoO_4 and disphenoidal SbO_4 moieties. They exhibit characteristic Sb^{3+} photoluminescence.

Keywords: Rare earth molybdoantimonite; Solid-state synthesis; X-ray diffraction; Crystal structure; Crystal growth; Luminescence

1. Introduction

There has been an upsurge of interest in the solid-state chemistry of tellurites, primarily for two reasons. One is their structural diversity arising out of coordination versatility of Te^{4+}, which exists in three asymmetric coordinations [1–5], namely, pyramidal TeO_3, disphenoid TeO_4, and square-pyramidal TeO_5. The other reason is their potential use as second-harmonic generating (SHG) materials. $Cs_2Mo_3TeO_{12}$, $Rb_4Mo_6Te_2O_{24}\cdot 6H_2O$, $BaMo_2TeO_9$ and $La_2MoTe_3O_{12}$ compounds are some of the many structurally diverse molybdotellurites realized in the quaternary A/Mo/Te/O (A = alkali, alkaline earth and lanthanide metals) system [6–8]. Molybdotellurites with non-centrosymmetric crystal structures, such as layered $Cs_2Mo_3TeO_{12}$ and $BaMo_2TeO_9$ compounds, exhibit SHG activity that is attributed to second-order Jahn-Teller (SOJT) distorted coordinations of Te^{4+} with stereoactive lone pair of electrons and d^0 transition metal ion, Mo^{6+}. Similarly tellurites containing other d^0 transition metal ions such as W^{6+}, V^{5+} have been reported to be SHG active [9]. However, it should be mentioned that several SHG inactive tellurites containing d^0 transition metal ions are known.

Sb^{3+} is isoelectronic with Te^{4+} and known to exhibit similar coordination versatility in oxides. Antimonites containing d^0 transition metal ions are rather few and are mostly ternary oxides [10–14]. For example, the molybdoantimonites known [15–22] are Sb_2MoO_6 $Sb_2Mo_{10}O_{31}$, $Na_4Sb_{12}Mo_5O_{35}$, $Sb_2W_{0.75}Mo_{0.25}O_6$, AMo_2SbO_8 (A = Cu, Li, K), $ASbMoO_5$ (A = K, Na), $Sb_{1.79}As_{0.21}MoO_6$, $Bi_{2-x}Sb_xMoO_6$ and $Bi_{1.1}Sb_{0.9}MoO_6$. Some of these compounds were studied from the point of view of luminescence and ferroelectric properties and no measurement of SHG activity was reported for non-centrosymmetric ones [15–18]. In view of our previous successful synthesis of several structurally diverse tungsto- and molybdotellurites [23] with a wide range of compositions and the scarcity of such interesting antimonite analogues, we have initiated the synthetic and structural investigation of several quaternary A/M/Sb/O (A = alkali, alkaline earth, lanthanide metals, etc.; M = Mo, W) systems. A number of new antimonites have been isolated in the trials patterned after synthesis of tellurite analogues. In this paper, we report the solid-state synthesis, single crystal X-ray structures and spectral properties of six isostructural $A_2Mo_4Sb_2O_{18}$ (A = Y(**1**), La(**2**), Nd(**3**), Sm(**4**), Gd(**5**) and Dy(**6**)) compounds containing discrete centrosymmetric $(Mo_4Sb_2O_{18})^{2-}$ anions. To our knowledge, these are the first examples of rare earth molybdoantimonites.

*Corresponding author. Fax: +91 44 22570509/4202.
E-mail address: kvsagar@iitm.ac.in (K. Vidyasagar).

0022-4596/$ - see front matter © 2007 Elsevier Inc. All rights reserved.
doi:10.1016/j.jssc.2007.03.024

2. Experimental

2.1. Synthesis and crystal growth

MoO_3, Sb_2O_3 and A_2O_3 (A = Y, La, Nd, Sm, Gd and Dy) oxides of high purity (>99.99%) were used for the solid-state synthesis and single crystal growth of $A_2(Mo_4Sb_2O_{18})$ compounds **1–6**, in evacuated sealed quartz tubes of 12 cm length and 1.4 cm diameter. A_2O_3 oxides were dried, by heating to 900 °C for 12 h, before use.

Polycrystalline samples of compounds **1–6** were synthesized quantitatively, on a scale of about 1 g, from stoichiometric mixtures of appropriate reactants. The reactant mixtures were heated first at 650 °C for 1 day, then at 700 °C for 4 days and finally cooled to room temperature over 1 day. For crystal growth, 1:6:1 molar mixtures of A_2O_3, MoO_3 and Sb_2O_3 were heated to 900 °C in 12 h and held at that temperature for 4 days and then cooled to room temperature over a period of 1 day. Compounds **1–6** were obtained as red block shaped single crystals (yield ~75%, based on Sb_2O_3), along with colourless MoO_3 crystals. The crystals of **1–6** were manually separated. It was also possible to isolate those crystals, by dissolving MoO_3 in ~2% Na_2CO_3 solution.

2.2. X-ray diffraction and crystal structure

The powder X-ray diffraction (XRD) patterns of compounds **1–6** were recorded on a Shimadzu XD-D1 powder diffractometer, using Cu$K\alpha$ ($\lambda = 1.5406$ Å) radiation. The monophasic nature of all six compounds was verified by comparing their powder XRD patterns with those simulated, using the LAZY-PULVERIX programme [24], on the basis of their single crystal X-ray structures. Single crystals of the compounds **1–6**, suitable for XRD, were selected and mounted on thin glass fibres with epoxy glue and optically aligned on a Bruker APEX II charge-coupled device X-ray diffractometer using a digital camera. Intensity data were measured at 25 °C, using graphite monochromated Mo$K\alpha$ radiation ($\lambda = 0.7103$ Å) from a sealed tube and monocapillary collimator. APEX II software (Bruker AXS) was used for preliminary determination of the cell constants and data collection control [25]. The determination of integral intensities and global refinement were performed using SAINT+ (Bruker AXS) with a narrow-frame integration algorithm. A semiempirical absorption correction [26] was subsequently applied using SADABS. SHELXTL programme was used for space group determination (XPREP), direct methods structure solution (XS), and least-squares refinement (XL). The graphic programmes [27,28] DIAMOND and ORTEP were used to draw the structures. The observed systematic absences of the data indicated $C2/c$ and Cc as the possible space groups. Both the space groups turned out to be good for successful structure solution and refinement. However, the centrosymmetric $C2/c$, with lower values of weighted R factor, was preferred [29]. The structure was solved by direct methods and refined by full-matrix least squares on F^2.

For yttrium (**1**) compound, the positions of the metal atoms were first located and refined. The subsequent Fourier difference maps led to location of oxygen atoms. Structures of compounds **2–6** were modelled, starting with the refined positional parameters of **1**, and only yttrium was appropriately replaced. All atoms were refined anisotropically in the case of five compounds, **1–4** and **6**. The final Fourier difference maps did not show any chemically significant feature and the peaks with an electron density of >1 e/Å^3 were found to be ghosts. Pertinent crystallographic data are presented in Table 1. For isostructural gadolinium (**5**) compound, X-ray data suffers from severe absorption; its final structure refinement, with weighted residual factor of 11.7% and residual peak of 8.9 e/Å^3 in the difference Fourier map, was not satisfactory. Its unit cell parameters, in monoclinic $C2/c$ space group, are the following: $a = 12.9309(3)$, $b = 14.17776(2)$, $c = 10.7208(3)$ Å, $\beta = 123.722(2)^\circ$ and $V = 1634.73(7)$ Å^3.

3. Characterization

Infrared, UV/Vis absorption and fluorescence spectra were recorded at room temperature on a Nicolet 6700 FT-IR, Cary 5E Varian UV/Vis/NIR and Jobin Yvon Horiba Fluorolog-3 spectrophotometers, respectively. The samples were ground with dry KBr and pressed into transparent disks for recording infrared spectra (4000–400 cm^{-1}).

4. Results and discussion

Preliminary heating of stoichiometric mixture of reactants at melting temperature (~650 °C) of Sb_2O_3 for 1 day is found to be crucial for successful solid-state synthesis of polycrystalline samples of the six new molybdoantimonites $A_2(Mo_4Sb_2O_{18})$ **(1–6)**. The excess MoO_3 functioning as flux has facilitated the crystal growth of compounds **1–6**.

Powder XRD patterns of isostructural $A_2(Mo_4Sb_2O_{18})$ compounds (**1–6**) are similar and, as shown for compound 1 (Fig. 1), reasonably agree with the simulated ones. The values of unit cell volumes of **1–6** vary in accordance with the size of A^{3+} cations. These compounds have "zero-dimensional" structures containing A^{3+} cations and discrete tetramolybdodiantimonite anionic aggregates, $(Mo_4Sb_2O_{18})^{6-}$. The coordinations of A^{3+}, Mo^{6+} and Sb^{3+} ions are, respectively, dodecahedral, tetrahedral and disphenoidal.

The structural features of compounds, **1–6** are discussed by taking yttrium (**1**) compound as an example. The asymmetric unit content is half of one formula unit, represented by one antimony (Sb), two molybdenum (Mo(1) and Mo(2)), and nine oxygen (O(1)–O(9)) atoms in general positions and two yttrium (Y(1) and Y(2)) atoms on crystallographic two-fold axes. $(Mo_4Sb_2O_{18})^{6-}$ anionic unit sits on crystallographic inversion centres and consists

Table 1
Pertinent crystallographic data for $A_2Mo_4Sb_2O_{18}$ (A = Y(**1**), La(**2**), Nd(**3**), Sm(**4**), Dy(**6**)) compounds

Compound	1	2	3	4	6
Formula	$Y_2Mo_4Sb_2O_{18}$	$La_2Mo_4Sb_2O_{18}$	$Nd_2Mo_4Sb_2O_{18}$	$Sm_2Mo_4Sb_2O_{18}$	$Dy_2Mo_4Sb_2O_{18}$
Formula weight	1093.08	1193.08	1203.74	1215.96	1240.26
Crystal system	Monoclinic	Monoclinic	Monoclinic	Monoclinic	Monoclinic
a (Å)	12.8794(3)	13.1681(3)	13.0470(5)	12.9825(2)	12.8949(3)
b (Å)	14.0580(2)	14.5778(3)	14.3708(5)	14.2664(3)	14.0912(3)
c (Å)	10.6608(3)	10.9414(2)	10.8362(4)	10.7922(2)	10.6833(4)
α (°)	90	90	90	90	90
β (°)	123.765(1)	123.453(1)	123.584(2)	123.738(2)	123.759(1)
γ (°)	90	90	90	90	90
V (Å^3)	1604.65(7)	1752.39(6)	1692.59(2)	1662.23(2)	1613.88(8)
Space group (No.)	$C2/c$ (15)	$C2/c$ (15)	C2/c (15)	C2/c (15)	$C2/c$ (15)
Z	4	4	4	4	4
ρ_{calcd} (g/cm^3)	4.525	4.522	4.724	4.859	5.104
λ(Mo$K\alpha$) (Å)	0.71073	0.71073	0.71073	0.71073	0.71073
μ(Mo$K\alpha$) (mm^{-1})	13.567	10.643	12.106	13.145	15.522
Total reflections	12773	13743	13611	14393	13330
Independent reflections	2410	2683	2557	2542	2500
$R^{[a]}$	0.0213	0.0215	0.0204	0.0185	0.0233
$R_w^{[b]}$	0.0447	0.0565	0.0519	0.0417	0.0544

[a] $R = \Sigma||F_o|-|F_c||/\Sigma|F_o|$; [b] $R_w = [\Sigma w(|F_o|^2-|F_c|^2)^2/\Sigma w(|F_o|^2)^2]^{1/2}$.

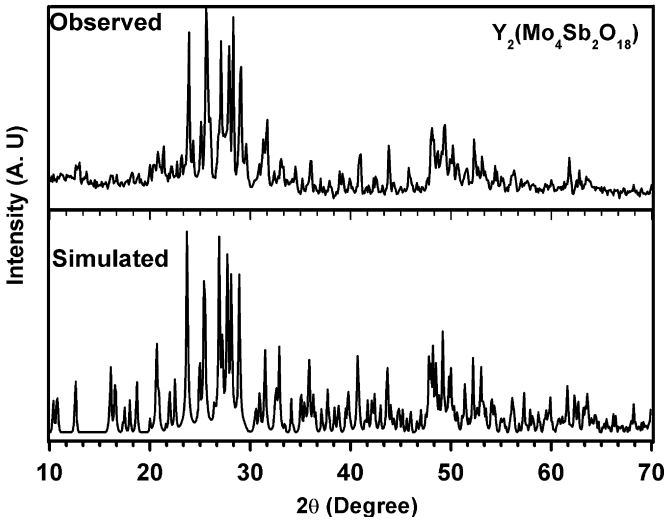

Fig. 1. Observed (top) and simulated (bottom) XRD powder patterns of $Y_2(Mo_4Sb_2O_{18})$.

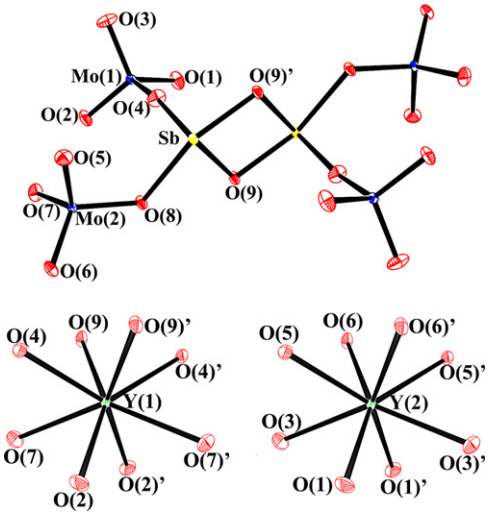

Fig. 2. ORTEP diagram of $(Mo_4Sb_2O_{18})^{6-}$ anion (top) and dodecahedral coordination (bottom) of Y(1) and Y(2) in $Y_2(Mo_4Sb_2O_{18})$. Thermal ellipsoids are drawn at the 50% probability level.

of two disphenoidal SbO_4 and four tetrahedral MoO_4 moieties (Fig. 2). Mo(1) and Mo(2) are tetrahedrally bonded to O(1)–O(4) and O(5)–O(8) sets of oxygen atoms, respectively. In disphenoidal SbO_4 unit, Sb atom forms axial bonds with O(4) and O(9) and equatorial bonds with O(8) and inversion-related O(9)'. This disphenoidal SbO_4 unit is edge-connected to its inversion-related one, through O(9) and O(9)', and corner-connected to two MoO_4 tetrahedra, through O(4) and O(8). All oxygen atoms, except O(8), are involved in bonding to yttrium atoms (Fig. 2). The discrete nature and location of centrosymmetric $(Mo_4Sb_2O_{18})^{6-}$ anions in the unit cell is evident from the unit cell diagrams (Fig. 3). The arrangement of A^{3+} ions could be described as corrugated layers parallel to ac planes. The values of bond lengths (Table 2) and angles of SbO_4, MoO_4 and AO_8 polyhedra compare well with those reported [17,20,30] in the literature. The values of axial Sb–O bond lengths are higher than those of the corresponding equatorial ones. Mo(1)–O(4) and Mo(2)–O(8) bonds are longer than other Mo–O bonds. The bond valence sums [31] are found to be in the ranges of 5.85–6.15, 3.00–3.50 and 3.25–3.50 for Mo^{6+}, Sb^{3+} and A^{3+} ions, respectively, in compounds **1–6**. These centrosymmetric compounds are presumed to be SHG inactive.

Compounds **1–6** have structural or compositional similarities with the layered molydoantimonites, NaMoSbO_5, AMo_2SbO_8 (A = Li, K, Cu) and molybdotellurite,

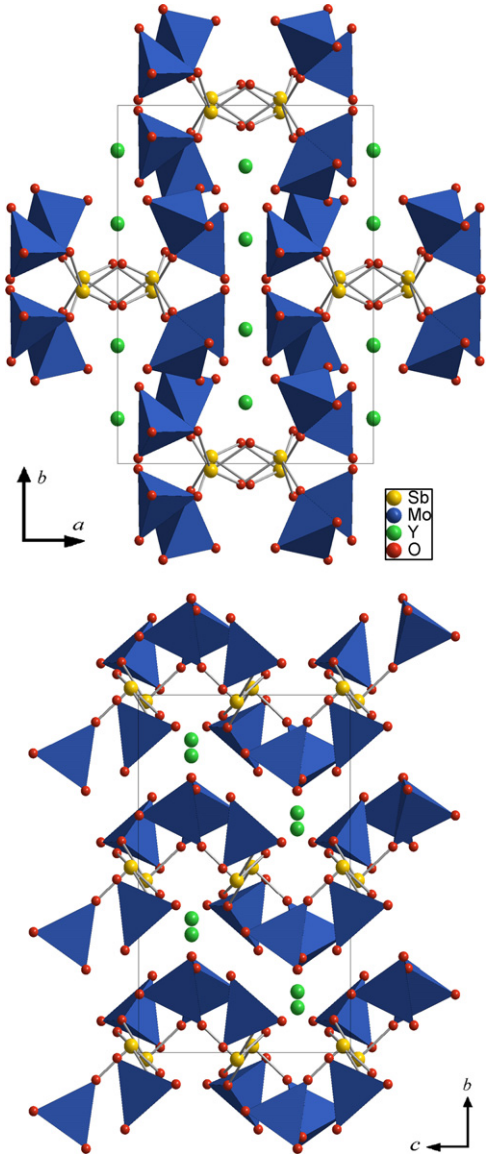

Fig. 3. Polyhedral representation of the unit cell of $Y_2(Mo_4Sb_2O_{18})$ viewed along (bottom) *a*- and (top) *c*-axes. MoO_4 tetrahedra are shaded in blue.

Table 2
Bond lengths (Å) for $A_2(Mo_4Sb_2O_{18})$ (A = Y(**1**), La(**2**), Nd(**3**), Sm(**4**) and Dy(**6**)) compounds

Compound	1	2	3	4	6
Sb–O(4)	2.283(2)	2.338(3)	2.315(3)	2.299(3)	2.277(3)
Sb–O(8)	1.982(2)	1.972(3)	1.974(3)	1.982(3)	1.978(4)
Sb–O(9)	2.067(2)	2.063(3)	2.064(3)	2.062(3)	2.067(3)
Sb–O(9)'	1.990(2)	1.992(3)	1.992(3)	1.991(3)	1.992(4)
Mo(1)–O(1)	1.725(2)	1.723(3)	1.723(3)	1.725(3)	1.728(4)
Mo(1)–O(2)	1.749(3)	1.749(3)	1.751(3)	1.751(3)	1.748(4)
Mo(1)–O(3)	1.766(2)	1.764(3)	1.765(3)	1.762(3)	1.763(4)
Mo(1)–O(4)	1.817(2)	1.809(3)	1.811(3)	1.814(3)	1.821(3)
Mo(2)–O(5)	1.740(3)	1.726(3)	1.732(3)	1.734(4)	1.737(4)
Mo(2)–O(6)	1.729(3)	1.731(3)	1.728(3)	1.730(3)	1.729(4)
Mo(2)–O(7)	1.746(3)	1.744(3)	1.745(3)	1.742(3)	1.743(4)
Mo(2)–O(8)	1.811(3)	1.816(3)	1.815(3)	1.809(3)	1.812(4)
A(1)–O(2) × 2	2.313(2)	2.446(3)	2.391(3)	2.360(3)	2.323(4)
A(1)–O(4) × 2	2.341(2)	2.493(3)	2.434(3)	2.402(3)	2.353(3)
A(1)–O(7) × 2	2.441(3)	2.534(3)	2.492(3)	2.474(3)	2.445(4)
A(1)–O(9) × 2	2.336(2)	2.500(3)	2.436(3)	2.408(3)	2.350(3)
A(2)–O(1) × 2	2.384(2)	2.501(3)	2.455(3)	2.429(3)	2.390(4)
A(2)–O(3) × 2	2.318(2)	2.473(3)	2.411(3)	2.384(3)	2.330(4)
A(2)–O(5) × 2	2.335(2)	2.504(3)	2.438(3)	2.406(3)	2.349(4)
A(2)–O(6) × 2	2.393(2)	2.508(3)	2.462(3)	2.434(3)	2.397(4)

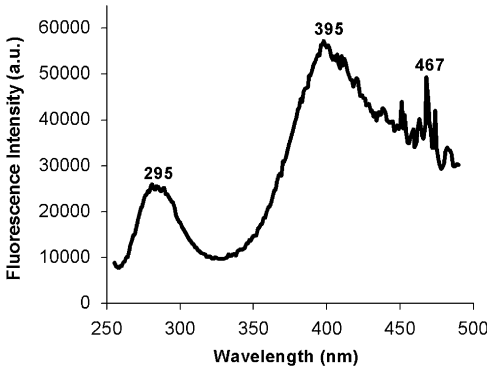

Fig. 4. Room temperature solid-state emission spectrum of $Y_2(Mo_4Sb_2O_{18})$, under excitation at $\lambda_{ex} = 250$ nm.

$BaMo_2TeO_9$. Disphenoidal SbO_4 and tetrahedral MoO_4 moieties constitute, as in **1–6**, the anionic Mo–Sb–O framework [20] of $NaMoSbO_5$. Compounds **1–6** and AMo_2SbO_8 (A = Li, K, Cu) have Mo^{6+} and Sb^{3+} content in the ratio of 2:1. The structures of $LiMo_2SbO_8$ and $CuMo_2SbO_8$ consist of corrugated perovskite-like layers of MoO_6 octahedra, with the disphenoidally coordinated Sb^{3+} and octahedrally coordinated Li^+/Cu^+ ions segregated on opposite sides of each layer [19]. In non-centrosymmetric KMo_2SbO_8, $[Mo_2SbO_8]^-$ anionic layers are built from square-pyramidal SbO_5, MoO_6 and MoO_5 polyhedra and interleaved with K^+ ions [19]. $BaMo_2TeO_9$ has similar AMo_2XO_9 ($A = Ba^{2+}/A^{3+}$; $X = Te^{4+}/Sb^{3+}$) empirical formula [7] of **1–6** but non-centrosymmetric structure, with octahedral MoO_6 and pyramidal TeO_3 moieties constituting the layered anionic framework of $[Mo_2TeO_9]^{2-}$.

The infrared spectra of compounds **1–6** have some common features that could be reasonably accounted for. The peaks at 935 and 857 cm^{-1} are due to Mo–O stretching vibrations, whereas peak at 741 cm^{-1} is due to Mo–O–Mo vibration [8,17,32]. The peaks at 571 and 472 cm^{-1} are ascribed to Sb–O–Sb vibrations [33].

UV–vis absorption spectrum of compound **3** contains maximum number of peaks at 250, 350, 500, 583, 687, 741 and 753 nm. Compound **6** has the first three absorption bands and also a peak at 753 nm, whereas compounds **1**, **2** and **4** have only the first three absorption bands. Compound **5** shows only the last two peaks. The study of emission spectra of these compounds was confined to excitations at the wavelengths of absorption bands, 250, 350 and 500 nm. As shown in the emission spectrum (Fig. 4) of compound **1**, all six compounds exhibit, under excitation at 250 nm, two broad emission bands around

295 and 395 nm and another sharp one at 467 nm. The broad bands are similar to those reported [34,35] for Sb^{3+}-doped LPO_4 (L = Sc, Lu, Y). Accordingly, the excitation band at 250 nm is assigned to the allowed $^1S_0$–$^3P_1$ transition and the resulting broad emission bands could be attributed to the $^3P_{1,0}$–$^1S_0$ transitions of Sb^{3+}. Only the last two emissions, namely those at 395 and 467 nm, have been observed on excitation at 350 nm. When excited at 500 nm, no emission was observed up to 800 nm. At present, the origin of 467 nm emissions is not clear. Emission in 500–800 nm range, normally ascribed to molybdate, is not observed [36].

4. Concluding remarks

Six, new, isostructural $A_2(Mo_4Sb_2O_{18})$ (A = Y, La, Nd, Sm, Gd and Dy) molydoantimonites have been synthesized by solid-state reactions and structurally characterized, by single crystal XRD, to possess discrete centrosymmetric $(Mo_4Sb_2O_{18})^{6-}$ anions. They exhibit characteristic Sb^{3+} photoluminescence.

Acknowledgment

We thank the Department of Chemistry and Sophisticated Analytical Instrument Facility of our institute for single crystal X-ray data collection and spectroscopic measurements, respectively.

Appendix A. Supplementary materials

Supplementary data associated with this article can be found in the online version at doi:10.1016/j.jssc.2007.03.024.

References

[1] J.D. Woodward, T.E. Albrecht-Schmitt, J. Solid State Chem. 178 (2005) 2922–2926.
[2] J.D. Woodward, P.M. Almond, T.E. Albrecht-Schmitt, J. Solid State Chem. 177 (2004) 3971–3976.
[3] M.P. Minimol, K. Vidyasagar, Inorg. Chem. 44 (2005) 9369–9373.
[4] O. Noguera, P. Thomas, O. Masson, J.C. Champarnaud-mesjard, Z. Kristallogr. 218 (2003) 293–294.
[5] W. Klein, J. Curda, E.M. Peters, M. Jansen, Z. Anorg. Allg. Chem. 631 (2005) 2893–2899.
[6] B. Vidyavathy, K. Vidyasagar, Inorg. Chem. 37 (1998) 4764–4774.
[7] H.S. Ra, K.M. Ok, P.S. Halasyamani, J. Am. Chem. Soc. 125 (2003) 7764–7765.
[8] Y.L. Shen, H.L. Jiang, J. Xu, J.G. Mao, K.W. Cheah, Inorg. Chem. 44 (2005) 9314–9321.
[9] P.S. Halasyamani, Chem. Mater. 16 (2004) 3586–3592.
[10] H. Fjellvaag, A.N. Christensen, J Pannetier, Acta Chem. Scand. 44 (1990) 975–977.
[11] V.I. Popolitov, Neorg. Mater. 28 (1992) 1497–1502.
[12] V.I. Popolitov, G.F. Plakhov, Iz. Akad. Nauk SSSR, Neorg. Mater. 24 (1988) 348–350.
[13] N.V. Rannev, B.M. Shchedrin, Y.N. Venevtsev, Ferroelectrics 13 (1976) 523–525.
[14] K.M. Ok, N.S.P. Bhuvanesh, P.S. Halasyamani, J. Solid State Chem. 161 (2001) 57–62.
[15] (a) A. Laarif, F.R. Theobald, H. Vivier, A.W. Hewat, Z. Kristallogr. 167 (1984) 117–124;
(b) A. Laarif, A. Hewat, F. Theobald, H. Vivier, J. Appl. Crystallogr. 16 (1983) 143;
(c) A. Castro, R. Enjalbert, J. Galy, Acta Crystallogr. Sect. C C53 (1997) 1526–1529;
(d) M. Parmentier, A. Courtois, Ch. Gleitzer, Bull. Soc. Chim. Fr. 1 (1974) 75–77.
[16] M. Parmentier, C. Gleitzer, A. Courtois, J. Protas, Acta Crystallogr. Sect. B B35 (1979) 1963–1967.
[17] Y. Wang, H. Zhang, R. Sun, C. Huang, X. Yu, J. Solid State Chem. 178 (2005) 902–907.
[18] R. Enjalbert, J. Galy, A. Castro, S. Lidin, R. Withers, G.V. Tendeloo, Solid State Sci. 5 (2003) 721–724.
[19] (a) H. Szillat, H. Mueller-Buschbaum, Z. Naturforsch. B50 (1995) 717–720;
(b) K.H. Lii, B.R. Chueh, J. Solid State Chem. 93 (1991) 503–509;
(c) K.H. Lii, B.R. Chueh, S.L. Wang, J. Solid State Chem. 86 (1990) 188–194.
[20] (b) Y. Wang, H. Zhang, C. Huang, Q. Sun, X. Yu, Inorg. Chem. Commun. 7 (2003) 21–23.
[21] G. Adiwidjaja, K. Friese, K.-H. Klaska, J. Schluter, M. Czank, Z. Kristallogr. 215 (2000) 529–535.
[22] P. Begue, R. Enjalbert, A. Castro, J. Solid State Chem. 159 (2001) 72–79.
[23] B. Vidyavathy, Ph.D. Thesis, Indian Institute of Technology Madras, Chennai, India, 2000.
[24] K. Yvon, W. Jeitschko, E. Parthe, J. Appl. Crystallogr. 10 (1977) 73–74.
[25] G.M. Sheldrick, SHELXTL, Bruker AXS, Inc., Madison, WI, 1997.
[26] G.M. Sheldrick, SADABS, University of Göttingen, Göttingen, Germany, 2004.
[27] W.T. Pennington, DIAMOND, J. Appl. Crystallogr. 32 (1999) 1028–1029.
[28] C.K. Johnson, ORTEP, Oak Ridge National Laboratory, Oak Ridge, TN, 1976.
[29] R.E. Marsh, Acta Crystallogr. Sect. B B42 (1986) 193–198.
[30] M.J. Bennett, F.A. Cotton, P. Legzdins, S. Lippard, Inorg. Chem. 7 (1968) 1770–1776.
[31] (a) N.E. Brese, M. O'Keeffe, Acta Crystallogr. B47 (1991) 192–197;
(b) I.D. Brown, D. Altermatt, Acta Crystallogr. Sect. B B41 (1985) 244–247.
[32] A.P.A. Marques, D.M.A. Melo, C.A. Paskocimas, P.S. Pizani, M.R. Joya, E.R. Leite, E. Longo, J. Solid State Chem. 179 (2006) 658–665.
[33] I.L. Botto, E.J. Baran, C. Cascales, I. Rasines, S.R. Puche, J. Phys. Chem. Solids 52 (1991) 431–434.
[34] J. Grafmeyer, J.C. Bourcet, J. Janin, J.P. Denis, J. Loriers, J. Lumin. 11 (1976) 369–380.
[35] E.W.J.L. Oomen, W.M.A. Smit, G. Blasse, Phys. Rev. B 37 (1988) 18–26.
[36] S. Shigeo, W.M. Yen, in: Phosphor Handbook, CRC Press, Boca Raton, FL, 1999, pp. 204–205.